Journal of Marine Systems 82 (2010) 187–194

Contents lists available at ScienceDirect

Journal of Marine Systems

journal homepage: www.elsevier.com/locate/jmarsys

Optimizing plankton survey strategies using Observing System Simulation Experiments

Pengfei Lin [a,b], Rubao Ji [b,*], Cabell S. Davis [b], Dennis J. McGillicuddy Jr. [c]

[a] State Key Laboratory of Numerical Modeling for Atmospheric Sciences and Geophysical Fluid Dynamics (LASG), Institute of Atmospheric Physics, Chinese Academy of Sciences, Beijing, 100029, China
[b] Department of Biology, Woods Hole Oceanographic Institution, Woods Hole, Massachusetts, 02543, USA
[c] Applied Ocean Physics & Engineering, Woods Hole Oceanographic Institution, Woods Hole, Massachusetts, 02543, USA

ARTICLE INFO

Article history:
Received 11 December 2009
Received in revised form 24 April 2010
Accepted 4 May 2010
Available online 12 May 2010

Keywords:
Observing System Simulation Experiments
Plankton
Optimization
Variance quadtree

ABSTRACT

A major problem in biological oceanography is sparseness of data. Ocean observing systems are being developed to fill this need. Design of these systems can benefit from optimal sampling analysis applied to output of biological–physical models. This study describes a method for optimizing plankton surveys through the use of Observing System Simulation Experiments (OSSEs). Using a coupled physical–biological hindcast simulation for 1999 as "truth", we applied the variance quadtree (VQT) algorithm to determine the locations of a fixed number of samples to reduce error. The optimized sampling process derived by the VQT algorithm is significantly better (at 95% confidence level) than simple random sampling. The relationship between root mean square error (RMSE) and number of samples allows one to balance the number of samples and the expected error, aiding the design of ocean observing systems. Compared with an existing sampling strategy used in the Gulf of Maine region, a fixed VQT-derived sampling strategy for *Pseudocalanus* alone can reduce expected errors by 20% on the annual average (range from 15% to 23%). While sampling for combination of two variables (adult *Pseudocalanus* and phytoplankton), the errors are modestly reduced by an annual average of 7% (range from −4% to 14%), suggesting that the ongoing operational observing strategy is close to optimal for multi-constituent sampling. The VQT-derived sampling stations are more densely (sparsely) spaced in areas having larger (lower) variance in the quantity of interest. Sampling strategies differ for *Pseudocalanus* and phytoplankton, reflecting differences in the statistics of their distributions. This kind of information can be used for directed sampling in the real ocean, which must grapple with multiple physical and biological properties that vary on different scales. This methodology can contribute to optimal sampling of biological–physical properties by ocean observing systems.

1. Introduction

Marine ecosystem dynamics are characterized by multiple species interacting with each other and their chemical and physical environment over multiple temporal and spatial scales (e.g. Haury et al., 1978; Davis et al., 1992; Davis and McGillicuddy, 2006; Zhang and Richardson, 2007). It is now widely recognized that existing data streams must be expanded to provide more accurate estimates of ecosystem status and to provide information for model simulation and prediction. New ocean observing systems are being developed to meet this need, but their designs are typically based more on expert knowledge than quantitative assessment and optimization. The advent of new high-resolution coupled biological–physical models can help optimize sampling strategies used in ocean observing systems. The model-based Observing System Simulation Experiment (OSSE) is one possible solution to this problem (e.g. Arnold and Dey, 1986; Masutani et al., 2006; Zhang et al., 2009). OSSEs were originally developed in meteorology (e.g. Charney et al., 1969) and have been considered for some time as a potentially important method for developing ocean observing systems (Smith, 1993; Robinson et al., 1998).

OSSEs involve the following three major components. 1) "Nature runs". A high-resolution model incorporating the best available knowledge on physics and biology is constructed, calibrated and validated. The outputs of model simulations are treated as "truth". 2) Simulated observations. Various sampling systems (such as shipboard surveys, fixed and profiling moorings, AUVs and gliders) are used to collect simulated data from the nature run. The "data" collected by the simulated sampling are analyzed in the same ways real data would be. 3) Quantification of sampling error. The error characteristics intrinsic to the simulated observations are assessed by comparing the difference between the original model output (i.e., "the truth") and the analyzed (in this case objectively mapped) data. The purpose of the OSSE is to minimize the expected error through optimizing the

* Corresponding author.
E-mail address: rji@whoi.edu (R. Ji).

0924-7963/$ – see front matter © 2010 Elsevier B.V. All rights reserved.
doi:10.1016/j.jmarsys.2010.05.005

sampling strategy (in this case the positions of the simulated observations in time and space).

OSSEs are now widely applied in meterological fields to assess observing systems for numerical weather prediction (e.g. Atlas, 1997; Masutani et al., 2009), the development of the data assimilation technology (e.g. Errico et al., 2007), as well as to help design future meteorological observing systems (e.g. Kuo et al., 1998; Bishop et al., 2001). OSSEs also have been increasingly used to help design sampling systems in physical oceanography. For instance, the optimal arrays of tide gauge and optimal locations of moorings in the tropical Atlantic have been designed using data assimilation method by McIntosh (1987) and Hackert et al. (1998), respectively. Hirschi et al. (2003) tested the design of a monitoring array for the Atlantic meridional overturning circulation in eddy-permitting ocean models. Recently, an observation array was designed and assessed in the tropical Indian Ocean to monitor intraseasonal and interannual variability in physical fields using an empirical orthogonal function and data assimilation approach (Oke and Schiller, 2007; Ballabrera-Poy et al., 2007; Vecchi and Harrison, 2007; Sakov and Oke, 2008). Some other studies have been focused on placing and managing fixed sensors for the coastal oceans (Frolov et al., 2008; Yildirim et al., 2009). Although OSSEs have been increasingly used to design sampling systems for physical properties, very few OSSEs have been used in biological oceanography. An earlier study by McGillicuddy et al. (2001) quantitatively assessed the synopticity of the broad-scale survey of copepod populations on Georges Bank (GB) using OSSEs as part of the Global Ocean Ecosystem Dynamics (GLOBEC) program. This study revealed that simple mapping error in terms of root mean square error (RMSE) could be as high as ~50% but reduced by about half when considering the effect of mean flow. This study has shown the advantage of using OSSEs to estimate the survey error and point out the value of optimizing survey strategy through simulated observations.

In this study, we explore the utility of OSSEs to optimize simulated observations for phytoplankton and copepod populations (*Pseudocalanus* spp.), using a recently developed high-resolution biological–physical model (Ji et al., 2009). The objectives of this study are to quantify expected error characteristics and their dependence on the total number of stations and their spatial/temporal distribution, based on the modeled spatio-temporal distribution pattern of plankton in the Gulf of Maine (GoM, see Fig. 1).

2. Data and methods

2.1. Data

We use results of a 3-dimensional (3D) high-resolution biological–physical coupled model to conduct OSSEs. The coupled model includes a hydrodynamic model called the finite-volume coastal ocean model (FVCOM, Chen et al., 2003, 2007), a 4-compartment (nitrogen–phytoplankton–µzooplankton–detritus, NPZD) lower food web model (to supply food for the copepod species), and a 4-stage (mean-age) concentration-based copepod population dynamics model (Hu et al., 2008; Ji et al., 2009).

For the hydrodynamic model, monthly averaged climatological temperature and salinity fields in December (retrieved from the National Oceanographic Data Center, NODC) were used as initial conditions, and the model was integrated over 1 yr using surface heat fluxes, vector wind and boundary forcing in 1999. Satellite-derived 5-day averaged sea surface temperature (SST) data were assimilated into the physical model. For the NPZD model, the initial distribution of nitrogen and phytoplankton were specified using the climatology in December derived from historical data; and the initial concentrations for µzooplankton and detritus were assumed to be homogeneous (Ji et al., 2008a,b). The copepod concentration was initialized based on the observed climatological distribution in December, with high and low concentrations in shallower and deep regions, respectively. The coupled FVCOM-NPZD captured the major seasonal and 3D spatial distributions of nutrient and phytoplankton across the GoM-GB region, based on comparisons with both SeaWiFS and water sample data, as a function of local and remote forcing (Ji et al., 2008a, b). Thus it can provide a good first-order approximation of food availability for the copepod model. The simulation used in this study is capable of representing the observed spatio-temporal pattern of *Pseudocalanus* spp. (Ji et al., 2009).

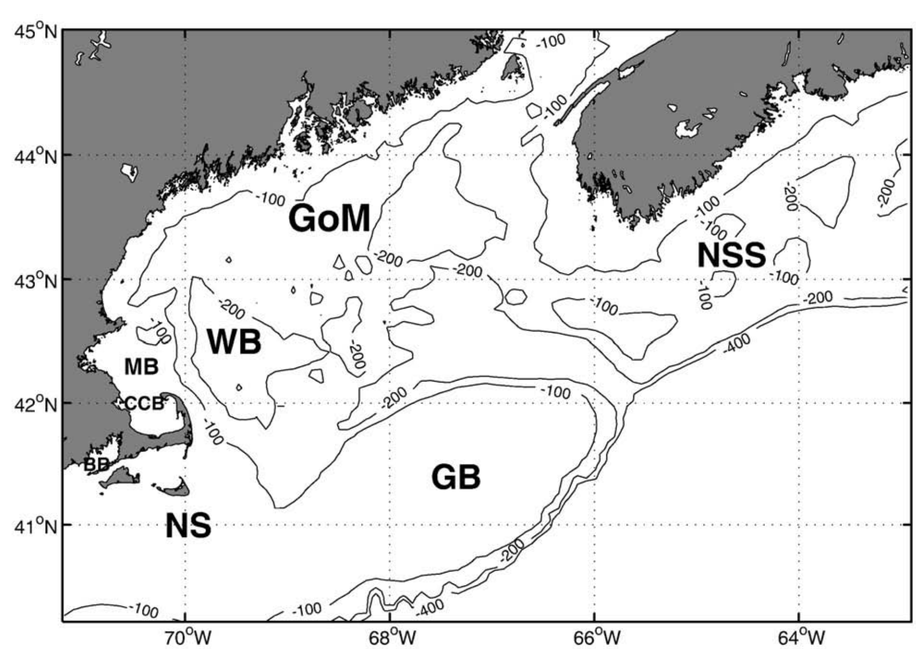

Fig. 1. The studied area, bathymetric isolines and some locations appeared in the paper. NS: Nantucket Shoals. GB: Georges Bank. WB: Wilkinson Basin. GoM: Gulf of Maine. NSS: Nova Scotian Shelf. MB: Massachusetts Bay. CCB: Cape Cod Bay. BB: Buzzards Bay.

2.2. Methods

In this study, we adopted a simple but computationally efficient algorithm called variance quadtree (VQT) algorithm for optimizing survey design. This algorithm was first introduced by McBratney et al. (1999) and improved by Minasny et al. (2007). The idea of VQT is based upon the principle of quadtree decomposition (i.e. divide the study area into quadrants or four equal sized strata). The stratum (sub-region) with maximum variance (calculated using the following equation) is chosen to conduct a subsequent quadtree decomposition, and the process is iterated until a certain threshold is reached (either the total number of strata or the minimum variance). The model variance for a chosen sub-region Q_h is defined as

$$Q_h = \sqrt{\frac{1}{2}\sum_{i=1}^{n_h}\sum_{j=1}^{n_h}\left[z(x_i)-z\left(x_j\right)\right]^2} \quad (1)$$

where n_h is the number of model gridpoints x_i and x_j in stratum h, and z is the study variable [see more details about the algorithm in Minasny et al. (2007)]. Note that Q_h is not normalized by n_h, so Q_h is affected by both the underlying variance and the number of gridpoints within each sub-region. In general, this algorithm places more sampling stations in areas where the spatial variance is large. The VQT algorithm considers the underlying variance in the quantity of interest in addition to geographical space, as suggested by Minasny and McBratney (2006). Although VQT requires complete access to the field being sampled, the scheme does not require prior knowledge of the spatial covariance function.

Although Minasny et al. (2007) gave examples using rectangular quadrants, they also mentioned that the VQT algorithm can be used with irregular geometries. The GoM domain is bounded by a rectangle, which includes land points and seaward boundaries. The domain is divided into quadrants using the VQT approach, and the variance within each sub-region whose variable of interest is not 'missing' (locating on the land or other places) based on Eq. (1) is computed. After the quadtree decomposition, the sampling point can be located in the center of a grid cell (center-selected) or in any random position within the cell (random-selected).

In this OSSE study, the surface fields of 3D high-resolution coupled model output served as the temporal–spatial continuous representation of reality ("truth"), and "virtual" phytoplankton and zooplankton samples were taken daily from the normalized model fields (normalized by subtracting annual mean and dividing by the standard deviation) using the VQT algorithm. The sampled data were mapped onto the 9 km × 9 km grids using an objective analysis method (OAX; He et al., 1997) based on Bretherton et al. (1976), with the same temporal and spatial correlation time scales used in McGillicuddy et al. (2001). Other interpolation algorithms (Matlab functions such as linear, cubic and V4) were tried for spatial mapping. The resulting spatial pattern is very similar to that based on OAX, and therefore the conclusion of this paper is robust with respect to the suite of interpolation algorithms that were tested. Our aim is to reduce the averaged RMSE over the entire sample domain. The averaged RMSE over the entire domain was computed by comparing the objective analysis of the simulated observations and the "truth".

3. Results

As a test case for optimizing the copepod sampling strategy in the GoM, we arbitrarily chose the modeled adult *Pseudocalanus* abundance field for June 8 in 1999 as "truth" (Fig. 2a). A total of 50 samples are taken based on the locations determined by the VQT algorithm. In general, the modified VQT method positions stations more densely in regions where the variance of *Pseudocalanus* abundance is higher, such as on Georges Bank (GB), to the west of Wilkinson Basin (WB), and west of Nantucket Shoals (NS). In contrast, in the regions such as in the central GoM and on the Nova Scotian Shelf (NSS, Fig. 1), where the gradient in abundance is lower, the stations are relatively sparse.

The general pattern of adult *Pseudocalanus* (Fig. 2b) from the simulated observation (after OAX mapping of the "data" from 50 stations) matches reasonably well with the "truth" shown in Fig. 2a. The absolute difference between the simulated distribution and the "truth" (Fig. 2d) shows relatively large error on GB, to the west of WB, west of NS and near the 400 m isobath, even with dense stations located there. In low-abundance areas with more uniform distributions, such as the NSS and the central GoM, the absolute error is relatively small, even with sparse stations.

The effectiveness of the modified VQT algorithm can be quantitatively estimated by comparing the results with simple random sampling, using the same number of stations (50) for both approaches. The random sampling was carried out 100 times, and the adult *Pseudocalanus* distribution was mapped for each sampling scenario using OAX (Fig. 2c). The general pattern of *Pseudocalanus* abundance from the ensemble mean of random sampling is also similar to the truth. The error in the regions with high spatial variability such as GB (Fig. 2d), appears to be about 0.5 (unit: dimensionless) larger than that using modified VQT algorithm (Fig. 2e, f), but smaller in regions with lower spatial variability (the center of GoM or NSS, Fig. 2e, f). These differences are attributable to the characteristics of the two sampling strategies: compared to the VQT-derived sampling, the relatively homogenous distribution of random stations results in more (less) stations in low- (high-) variance areas.

The VQT-derived sampling scheme can significantly decrease averaged RMSE of the *Pseudocalanus* survey in the region (Fig. 3). The averaged RMSE for VQT is 0.62 (unit: dimensionless), significantly lower (reduced by 0.38, $p < 0.05$) than the mean RMSE of 1.0 estimated from random sampling cases.

One would expect the RMSE to decrease as the number of sampling stations increases. The RMSE of VQT-derived sampling drops quickly from >3 to <1 as the number of samples increases from 10 to 25, faster than the random sampling approach (Fig. 4, top panel). The decrease of RMSE becomes more gradual as the number of samples continues to increase using both approaches, but the ensemble mean of RMSE for random sampling is larger than the VQT-based sampling when the sampling number exceeds 25. As the number of samples goes beyond 100, the RMSE begins to level off and approaches 0.4, suggesting that all the sub-regions have similar variance. The above analysis is only for distribution of adult *Pseudocalanus* in a specific day (a snapshot). Similar analysis was done for annual mean and standard deviation of RMSE for year 1999 with varying number of total sampling stations. The result (Fig. 4, bottom panel) shows that the annual mean RMSE drops quickly from 1.4 to 0.5 when the total number of stations increased from 5 to 40, and the decrease of RMSE is much slower with additional stations. The standard deviation of RMSE decreased as the number of stations increased. This information could be useful in quantifying the marginal impact of additional stations on reducing RMSE. Comparison of the VQT sampling approach with a more traditionally designed oceanographic survey pattern follows below.

Due to the temporal variation of zooplankton distributions, changing sampling stations with time can also reduce sampling error. The daily VQT-derived survey position for adult *Pseudocalanus* was determined for the entire simulated year of 1999 (an animation can be found at the link http://www.whoi.edu/science/B/jilab/osse/Za_0115y09a.gif). Using the daily sample positions and the corresponding size of the sub-regions in each quadtree stratum, the density of sampling station in each grid cell (i.e. 1.0/number of unit grid in the sub-region) can be obtained. After averaging the daily density over 1999 in each grid cell, a spatial map of sampling intensity is obtained. The region with higher intensity is where survey efforts should be focused to obtain more accurate measurement of annual abundance patterns (Fig. 5a). Those regions are concentrated in

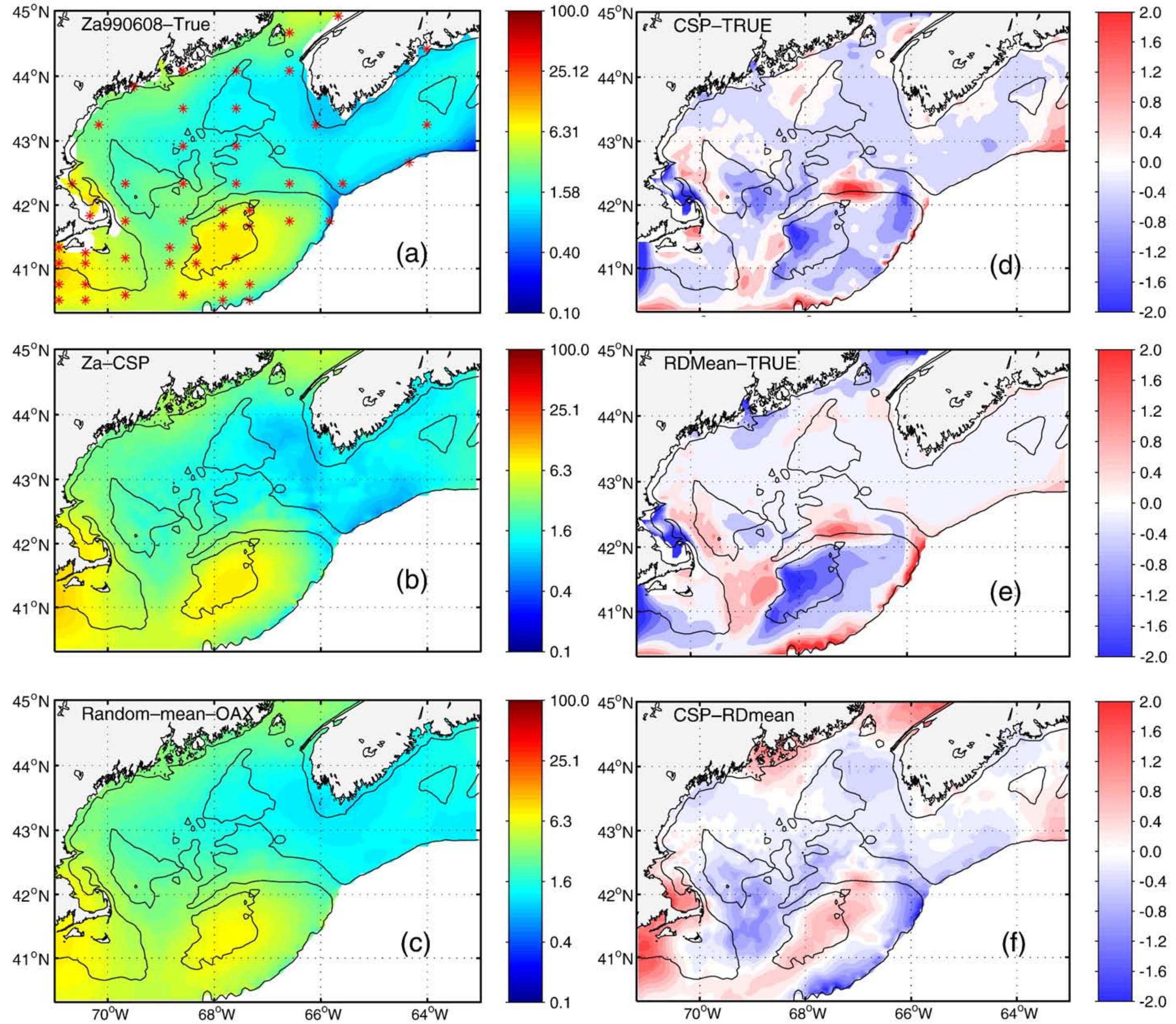

Fig. 2. (a) The modeled adult *Pseudocalanus* abundance field ("truth") on June 8 in 1999 (shaded, unit: dimensionless) and the 50 sample stations (red stars, center-selected) using VQT algorithm. (b) the OAX-mapped distribution of adult *Pseudocalanus* from the simulated observation using the VQT-based stations. (c) The ensemble mean field of objective analyses of 100 simulated surveys using random sampling with 50 stations (d) b–a; (e) c–a; (f)e–d.

Massachusetts Bay, Cape Cod Bay, Buzzards Bay**,** west WB and west GB. The sampling pattern changes when we applied the same analysis to the normalized distribution of daily phytoplankton in 1999 from the output of the NPZD model. (Fig. 5b). The key regions to survey are now located in the southwest GoM and the boundary between the east GoM and the Scotian Shelf.

We made a comparison with the survey strategy currently used for the Ecosystem Monitoring (EcoMon) program in the GoM by NOAA's National Marine Fisheries Service (NMFS), in which the stations are chosen using a random stratified design with a predefined set of 87 tiles within the GoM [Fig. 6, see Sherman (1980) and Meise and O'Reilly (1996) for program details and survey protocols]. The number of stations varied from survey to survey because some tiles could be missing in actual surveys. For comparison purpose we used the maximum number of stations (one station for each tile) for all the surveys in our analysis. The positions of 87 fixed VQT-derived stations for *Pseudocalanus* are more concentrated in the west GoM region; whereas NMFS survey stations have more stations located in the zone between 69.5 W and 67.5 W, and along the section around 66.5 W. Due to the difference in the spatial distribution between NMFS and VQT-derived stations, their averaged RMSEs for *Pseudocalanus* in the sample domain are different (Fig. 7). The VQT-derived RMSE ranges from 15 to 23% smaller than that based on NMFS stations.

4. Discussion

There could be many options for selecting the sampling positions (SPs) within each sub-region of the VQT algorithm. For the two approaches we used, over the course of a year, about 80% and 73% of averaged RMSEs of the center-selected SPs are smaller than that of randomly selected SPs for adult *Pseudocalanus* and phytoplankton, respectively (Fig. 8). Therefore, the center-selected SPs can be a

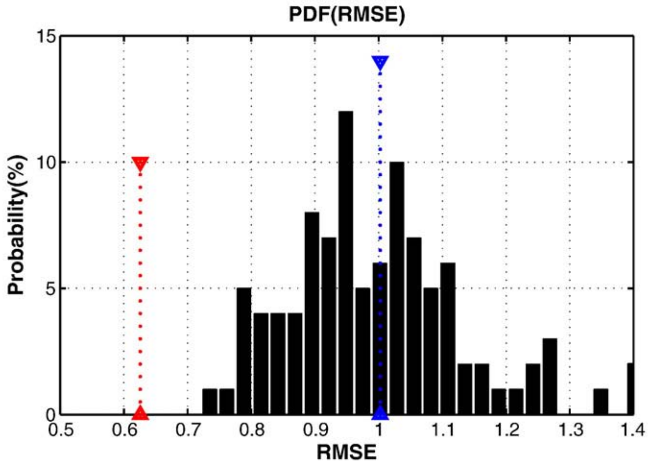

Fig. 3. The probability density function (PDF) of the averaged root mean square error (RMSE) of the spatial distribution of adult *Pseudocalanus*. Black bars indicate the PDF of averaged RMSE of 100 iterations of simple random sampling. The blue line is the mean RMSE of 100-times simple random sampling. The red line is the averaged RMSE for VQT-based sampling. 50 samples are used for both cases.

simple sampling strategy with reasonably low sampling errors. It may be possible to find other strategies with lower RMSEs by using higher order statistical moments of the distribution, but those aspects are left for future research.

It can be seen that the RMSE varies with time even for the same variable (Fig. 8), suggesting that the number of sampling stations needs to be adjusted to satisfy a specific RMSE threshold. For instance, more sampling stations for phytoplankton are probably needed to keep the RMSE low during spring bloom time period.

The high correlation (>0.9) between RMSE and averaged spatial gradient (Fig. 8) indicates the error can be related to the complexity of spatial gradient.

The sampling strategy discussed above focuses on few specific variables (surface adult *Pseudocalanus* or phytoplankton) only, with an understanding that, in reality, a sampling strategy for multiple variables is needed. In many cases, the spatial distribution of different biological fields at different depths could vary significantly. Thus it is necessary to explore whether the regions where sampling should be focused are different. A simple comparison of the spatial distribution of cumulative sampling frequency for phytoplankton and adult *Pseudocalanus* (Fig. 5a and b) reveals that the areas for focused sampling effort are not the same. For phytoplankton, more effort should be placed in the southwest Gulf of Maine and the boundary between the east GoM and the Scotian Shelf; whereas the effort for adult *Pseudocalanus* should be focused on in Massachusetts Bay, Cape Cod Bay, Buzzards Bay**,** west WB and west GB.

Our analysis suggests that the RMSE for *Pseudocalanus* is larger when more than one variable (e.g. both *Pseudocalanus* and phytoplankton) is considered when using the VQT method to design the survey strategy. Based on VQT-derived stations (Fig. 6b) for the combined variable (linear-combination of *Pseudocalanus* and phytoplankton), the averaged RMSE is reduced modestly (Fig. 7) when compared to the sampling strategy with only *Pseudocalanus* being considered. In some cases, such

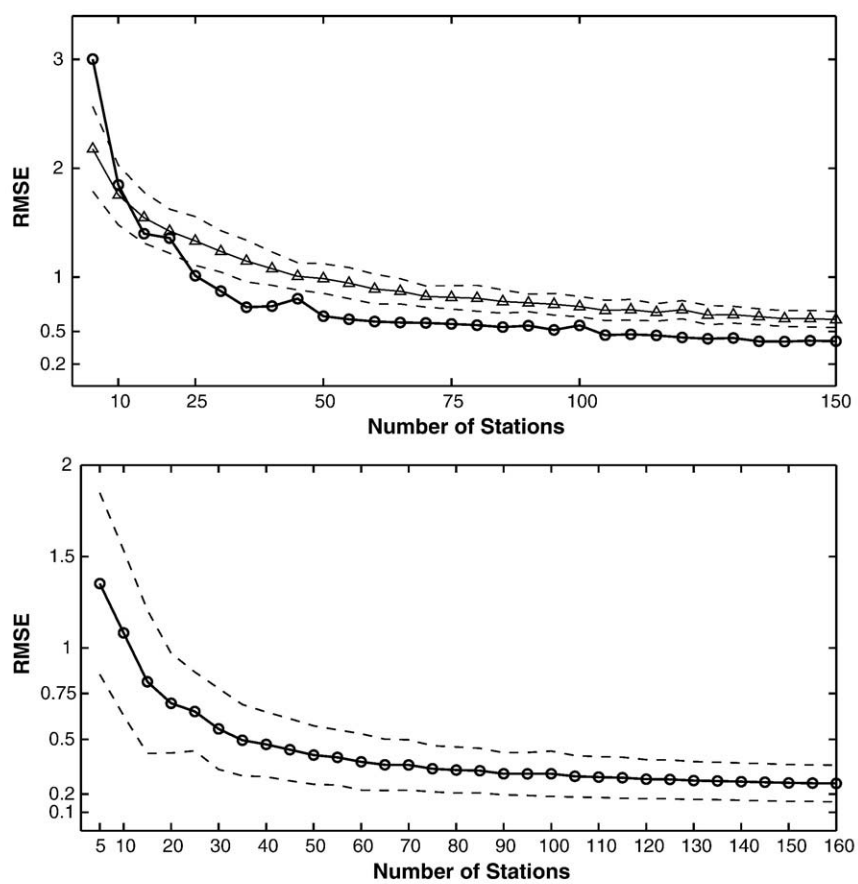

Fig. 4. (Upper panel) Averaged root mean square error (RMSE) versus number of stations. The black line with circles is spatial-averaged RMSE for VQT-based sample. The black line with triangles is the mean RMSE for simple random sampling repeated 100 times and the dashed line is 95% confidence interval about the mean RMSE of simple random sampling. (Bottom panel) Mean VQT-derived RMSE versus number of stations. The black line with circles is averaged RMSE over 1999 year for VQT-based sample. The dashed lines are mean RMSE±1STD of RMSE.

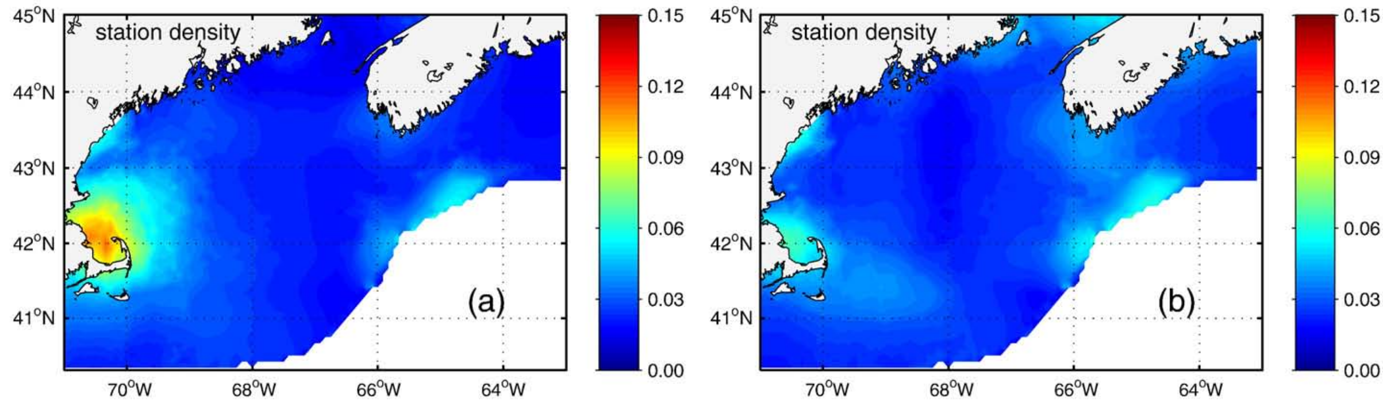

Fig. 5. (a) The VQT-derived sampling intensity for adult *Pseudocalanus*. (b) The same as (a) but for phytoplankton. The sampling intensity is defined as annual mean of station density in each grid (1.0/number of unit grid in the sub-region) in 1999. The daily number of stations is 50.

as January–February, the bimonthly mean RMSE based on VQT-derived stations is even larger than that based on the NMFS survey stations. Combining more variables in the VQT calculation (perhaps even non-dynamic variables such as depth) may cause the RMSE reduction to be even less significant, due to differences in the statistics of their spatial distribution. This indicates that the sampling strategy based on NMFS survey stations is essentially optimal in a multi-variable context.

Besides the seasonal scale, there are also interannual and decadal variabilities in plankton communities. In the GoM, phytoplankton and net primary production are characterized by strong interannual variability from 1998 to 2006 because of the influence of ocean freshening (Ji et al., 2007). In this study, only marine plankton at the seasonal scale is examined for optimizing the survey strategy. It is known that the key regions to monitor at different time scales (intraseasonal and seasonal–interannual) could be different due to distinct processes (e.g. Sakov and Oke, 2008). Further studies are needed to identify the key regions for sampling at interannual and decadal time scales in the GoM.

The model-based observing system design depends on the model performance (Sakov and Oke, 2008). Although the general spatio-temporal distribution pattern of biological variables can be captured reasonably well (Ji et al., 2009), there are differences between the modeled fields and reality. Typically, the modeled field is much smoother (less patchy) than the real distribution, due to the difficulties in capturing the sub-grid advection/diffusion processes and complex biological interactions not resolved by the model. There is also smoothing intrinsic to the OAX algorithm used to analyze the simulated data. Model bias can also be problematic in OSSE applications. Use of ensemble simulations may help reduce bias, but such improvements are left for future research. In any case, the present results must be interpreted with these caveats in mind. Even if the biological field used for the OSSEs is based on observations with reasonably high-resolution temporal and spatial coverage, such as satellite data, the same caution needs to be taken due to inevitable discrepancy between observation and reality (e.g. Stow et al., 2009).

5. Conclusions

In the paper, we focus on optimizing plankton sampling in the Gulf of Maine (GoM). The error is significantly smaller ($p<0.05$) and decreases more quickly with the number of sample stations derived by VQT than with simple random sampling. Furthermore, for long term measurements, the regions where sampling should be focused are found. For different variables, the corresponding focal regions can be different due to differences in their underlying variance properties. For the example distributions of phytoplankton, more effort should be placed in the

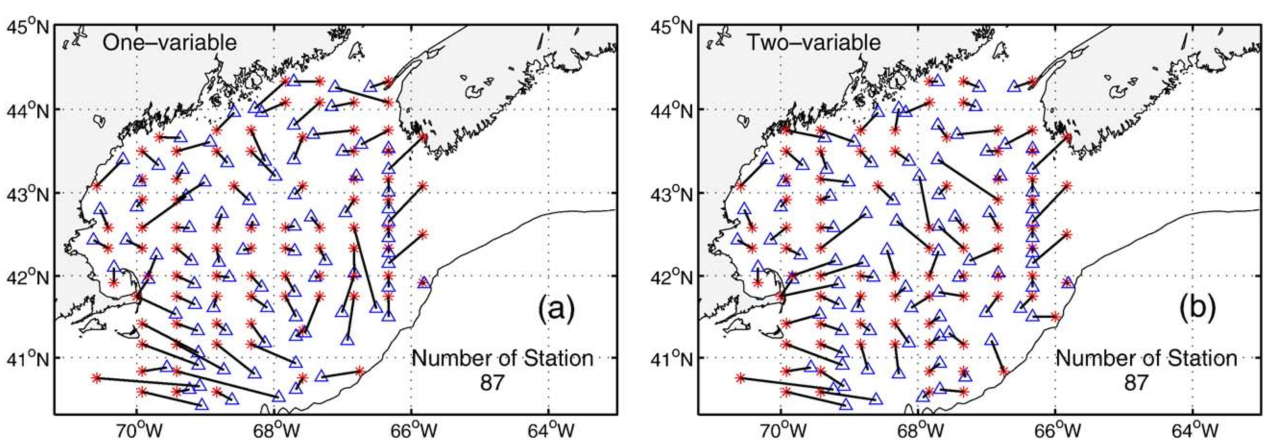

Fig. 6. The spatial distribution of 87 sample station positions based on (a) one variable (*Pseudocalanus*) and (b) linear-combination of two variables (*Pseudocalanus* and phytoplankton). Red stars are VQT-derived station positions based on the annual-averaged effort. Blue triangles are climatological annual station position from bimonthly NMFS (National Marine Fisheries Service) EcoMon station positions. The number of stations used for VQT sample is the same as that of NMFS stations in each case. The sample region for VQT is defined as the rectangle limited by the maximum and minimum longitude/latitude of NMFS EcoMon stations. The sample number of stations is shown at the bottom right on each panel. The black line is the pair pathway between VQT-derived stations and NMFS EcoMon stations based on the global shortest distance computed using Hungarian algorithm (Kuhn, 1956; Munkres, 1957).

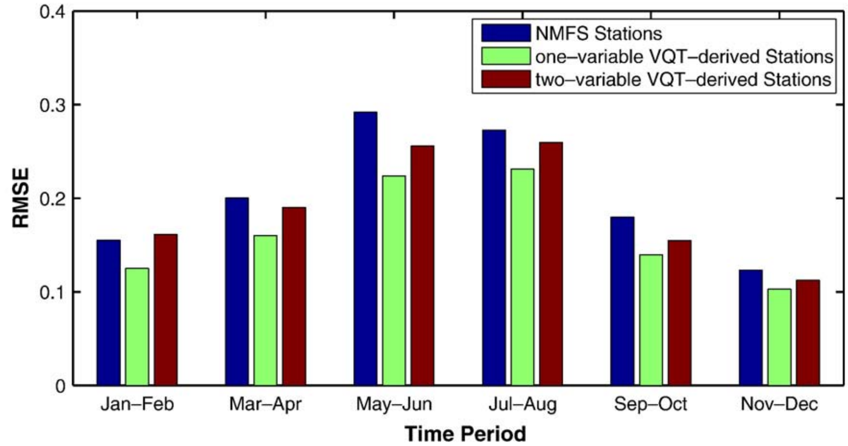

Fig. 7. The bimonthly-averaged normalized root mean square error (RMSE) for adult *Pseudocalanus* calculated by the climatological annual NMFS survey stations, fixed VQT-derived stations based on normalized *Pseudocalanus* and linear-combination (equal weight) of *Pseudocalanus* and phytoplankton, respectively. The number of VQT-derived station is the same as that of NMFS stations.

southwest GoM and the boundary between the east GoM and the Scotian Shelf; whereas the sampling effort for adult *Pseudocalanus* should be focused on the southwest Gulf of Maine. Compared with existing sampling strategy used in the Gulf of Maine region, the expected errors are reduced by 20% on the annual average (range from 15% to 23%) using sampling strategy informed by an ensemble of VQTs applied to the entire 1999 simulation for *Pseudocalanus* alone. While sampling for combination of two variables (adult *Pseudocalanus* and phytoplankton), the errors are modestly reduced by an annual average of 7% (range from −4% to 14%), suggesting that the ongoing operational observing strategy is close to optimal for multi-constituent sampling. Although we have limited the OSSE method to the distributions of plankton, it also can be applied to other biological variables in designing an optimized sampling array in future ocean observing systems. This

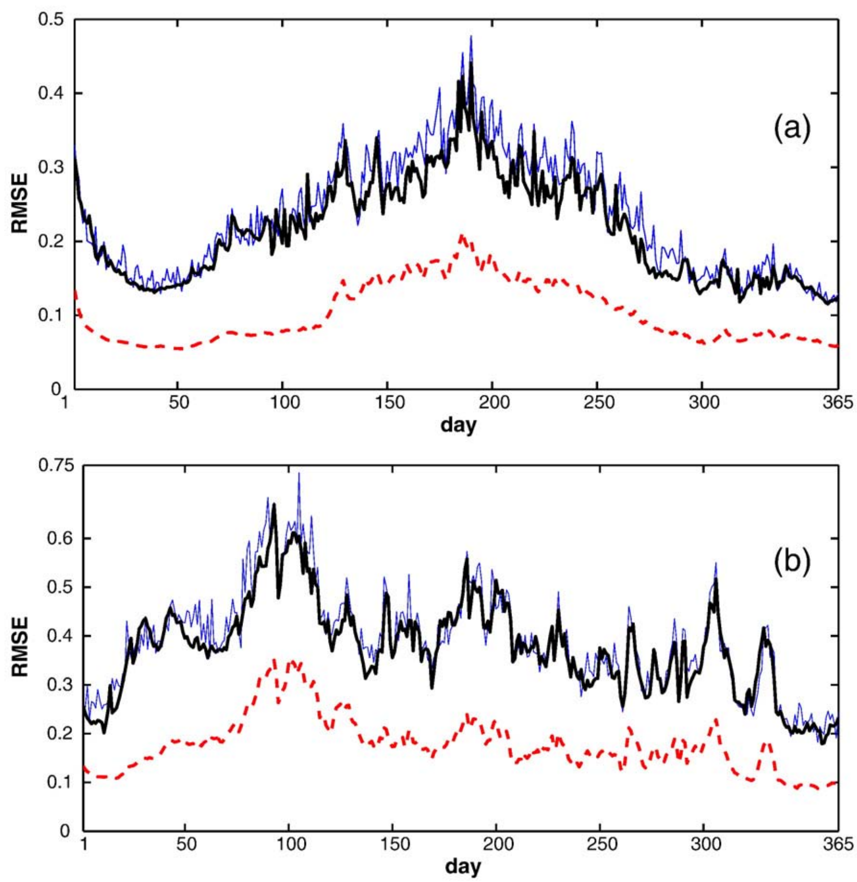

Fig. 8. (a) The time-varying spatial-averaged root mean square error (RMSE) of simulated observation for normalized adult *Pseudocalanus* over a year based on VQT-derived sampling stations (50 stations each day). (b) The same as (a) but for normalized phytoplankton. Black line is the averaged RMSE for center-selected sample positions. Blue line is the RMSE for random-selected sample positions. Red dashed line is the averaged spatial gradient.

study also provides a direction for optimizing sampling in space/time according to the previous survey information or validated-model simulation. This method can be extended to examine optimal overall sampling patterns for multiple variables and time scales.

Acknowledgments

This research was made possible by generous donations to the Woods Hole Oceanographic Institution by Hamilton James and The James Family Charitable Foundation, Robert and Lois Baylis, and Pi and Sally Chubb. Additional support includes: GLOBEC grants from the NSF (OCE0815838) and NOAA (NA17RJ1223) and the NSF (OCE0727033) to RJ and CSD; the NSF (OCE0934653) to DJM; and National Natural Science Foundation of China (40906012, 40775054) to PL. The Northeast Fisheries Science Center, Oceanography Branch, provided the NMFS survey information. J. Hare and D. Mountain reviewed an earlier draft of the manuscript.

References

Arnold Jr, C.P., Dey, C.H., 1986. Observing-systems simulation experiments: past, present, and future. Bulletin of the American Meteorological Society 67 (6), 687–695.

Atlas, R., 1997. Observing System Simulation Experiments. Proceedings of CGC/WMO Workshop, Geneva, pp. 7–9.

Ballabrera-Poy, J., Hackert, E., Murtugudde, R., Busalacchi, A.J., 2007. An Observing System Simulation Experiment for an optimal moored instrument array in the tropical Indian Ocean. Journal of Climate 20 (13), 3284–3299.

Bishop, C.H., Etherton, B.J., Majumdar, S.J., 2001. Adaptive sampling with the ensemble transform Kalman filter. Part I: theoretical aspects. Monthly Weather Review 129 (3), 420–436.

Bretherton, F.P., Davis, R.E., Fandry, C.B., 1976. A technique for objective analysis and design of oceanographic experiments applied to MODE-73. Deep Sea Research 23 (7), 559–582.

Charney, J., Halem, M., Jastrow, R., 1969. Use of incomplete historical data to infer the present state of the atmosphere. Journal of the Atmospheric Sciences 26 (5), 1160–1163.

Chen, C., Liu, H., Beardsley, R.C., 2003. An unstructured grid, finite-volume, three-dimensional, primitive equations ocean model: application to coastal ocean and estuaries. Journal of Atmospheric and Oceanic Technology 20 (1), 159–186.

Chen, C., et al., 2007. A finite volume numerical approach for coastal ocean circulation studies: comparisons with finite difference models. Journal of Geophysical Research 112, C03018.

Davis, C.S., McGillicuddy, D.J., 2006. Transatlantic abundance of the N2-fixing colonial cyanobacterium *Trichodesmium*. Science 312, 1517–1520.

Davis, C.S., Gallager, S.M., Solow, A.R., 1992. Microaggregations of oceanic plankton observed by towed video microscopy. Science 257 (5067), 230–232.

Errico, R.M., Yang, R., Masutani, M., Woollen, J., 2007. Estimation of some characteristics of analysis error inferred from an observation system simulation experiment. Meteorologische Zeitschrift 16, 695–708.

Frolov, S., Baptista, A., Wilkin, M., 2008. Optimizing fixed observational assets in a coastal observatory. Continental Shelf Research 28, 2644–2658.

Hackert, E.C., Miller, R.N., Busalacchi, A.J., 1998. An optimized design for a moored instrument array in the tropical Atlantic Ocean. Journal of Geophysical Research-Oceans 103 (C4), 7491–7509.

Haury, L.R., McGowan, J.A., Weibe, J.H., 1978. Patterns and processes in the time-space scales of plankton distributions. In: Steele, J.H. (Ed.), Spatial pattern in Plankton Communities. Plenum, New York 3, pp. 277–327.

He, I., Hendry, R. and Boudreau, G., 1997. OAX demonstration and test case. http://www.mar.dfo-mpo.gc.ca/science/ocean/coastal_hydrodynamics/Oax/oax.html#Changes.

Hirschi, J., Baehr, J., Marotzke, J., Stark, J., Cunningham, S., Beismann, J.O., 2003. A monitoring design for the Atlantic meridional overturning circulation. Geophysical Research Letters 30, 1413. doi:10.1029/2002GL016776.

Hu, Q., Davis, C.S., Petrik, C.M., 2008. A simplified age-stage model for copepod population dynamics. Marine Ecology Progress Series 360, 179–187.

Ji, R., et al., 2007. Influence of ocean freshening on shelf phytoplankton dynamics. Geophysical Research Letters 34 (24), L24607 10.1029/2007GL032010.

Ji, R., Davis, C., Chen, C., Beardsley, R., 2008a. Influence of local and external processes on the annual nitrogen cycle and primary productivity on Georges Bank: a 3-D biological–physical modeling study. Journal of Marine Systems 73 (1–2), 31–47.

Ji, R., Davis, C., Chen, C., Townsend, D., Mountain, D., Beardsley, R.C., 2008b. Modeling the influence of low-salinity water inflow on winter–spring phytoplankton dynamics in the Nova Scotian Shelf-Gulf of Maine region. Journal of Plankton Research 30 (12), 1399.

Ji, R., Davis, C.S., Chen, C., Beardsley, R.C., 2009. Life history traits and spatiotemporal distributional patterns of copepod populations in the Gulf of Maine-Georges Bank region. Marine Ecology Progress Series 384, 187–205.

Kuhn, H.W., 1956. Variants of the Hungarian method for assignment problems. Naval Research Logistics Quarterly 3, 253–258.

Kuo, Y.H., Zou, X., Huang, W., 1998. The impact of global positioning system data on the prediction of an extratropical cyclone: an Observing System Simulation Experiment. Dynamics of Atmospheres and Oceans 27 (1), 439–470.

Masutani, M., et al., 2006. Observing System Simulation Experiments at NCEP. US Dept. of Commerce,NCEP Office Note, 451: 34.

Masutani, M., et al., 2009. Observing System Simulation Experiments. Springer, pp. 1–29.

McBratney, B., Whelan, B.M., Walvoort, D.J.J., Minasny, B., 1999. A purposive sampling scheme for precision agriculture. Precision Agriculture 99 (2), 101–111.

McGillicuddy, D.J., et al., 2001. Evaluating the synopticity of the US GLOBEC Georges Bank broad-scale sampling pattern with observational system simulation experiments. Deep-Sea Research Part II 48 (1–3), 483–499.

McIntosh, P.C., 1987. Systematic design of observational arrays. Journal of Physical Oceanography 17 (7), 885–902.

Meise, C.J., O'Reilly, J.E., 1996. Spatial and seasonal patterns in abundance and age-composition of Calanus finmarchicus in the Gulf of Maine and on Georges Bank: 1977–1987. Deep-Sea Research Part II 43 (7–8), 1473–1501.

Minasny, B., McBratney, A.B., 2006. A conditioned Latin hypercube method for sampling in the presence of ancillary information. Computers and Geosciences 32 (9), 1378–1388.

Minasny, B., McBratney, A.B., Walvoort, D.J.J., 2007. The variance quadtree algorithm: use for spatial sampling design. Computers and Geosciences 33 (3), 383–392.

Munkres, J., 1957. Algorithms for the assignment and transportation problems. Journal of the Society for Industrial and Applied Mathematics 5 (1), 32–38.

Oke, P.R., Schiller, A., 2007. A model-based assessment and design of a tropical Indian Ocean mooring array. Journal of Climate 20 (13), 3269–3283.

Robinson, A.R., Lermusiaux, P.F.J., Sloan Iii, N.Q., 1998. Data assimilation. The sea 10, 541–594.

Sakov, P., Oke, P.R., 2008. Objective array design: application to the tropical Indian Ocean. Journal of Atmospheric and Oceanic Technology 25 (5), 794–807.

Sherman, K., 1980. MARMAP, a fisheries ecosystem study in the northwest Atlantic: fluctuations in ichthyoplankton–zooplankton components and their potential for impact on the system. In: Diemer, F.P., Verberg, F.J., Mirkes, D.Z. (Eds.), Advanced Concepts in Ocean Measurements for Marine Biology. Belle W. Baruch Institute for Marine Biology and Coastal Research. University of South Carolina Press, Columbia, pp. 3–37. 572.

Smith, N.R., 1993. Ocean modeling in a global ocean observing system. Reviews of Geophysics 31 (3), 281–317.

Stow, C.A., et al., 2009. Skill assessment for coupled biological/physical models of marine systems. Journal of Marine Systems 76 (1–2), 4–15.

Vecchi, G.A., Harrison, M.J., 2007. An Observing System Simulation Experiment for the Indian Ocean. Journal of Climate 20 (13), 3300–3319.

Yildirim, B., Chryssostomidis, C., Karniadakis, G.E., 2009. Efficient sensor placement for ocean measurements using low-dimensional concepts. Ocean Modelling 27, 160–173.

Zhang, Y., Richardson, J.S., 2007. Unidirectional prey–predator facilitation: apparent prey enhance predators' foraging success on cryptic prey. Biology Letters 3 (3), 348.

Zhang, W., Wilkin J. and Levin, J., 2009. Towards building an integrated observation and modeling system in the New York Bight using variational methods, Part II: representer-based observing system design. Submitted to Ocean Modelling.